



HAL
open science

Absorbing boundary conditions for water wave simulation in the vicinity of a solid body

Jose M. Orellana

► **To cite this version:**

Jose M. Orellana. Absorbing boundary conditions for water wave simulation in the vicinity of a solid body. 2020. hal-02962100v1

HAL Id: hal-02962100

<https://hal.science/hal-02962100v1>

Preprint submitted on 9 Oct 2020 (v1), last revised 29 May 2021 (v5)

HAL is a multi-disciplinary open access archive for the deposit and dissemination of scientific research documents, whether they are published or not. The documents may come from teaching and research institutions in France or abroad, or from public or private research centers.

L'archive ouverte pluridisciplinaire **HAL**, est destinée au dépôt et à la diffusion de documents scientifiques de niveau recherche, publiés ou non, émanant des établissements d'enseignement et de recherche français ou étrangers, des laboratoires publics ou privés.

Absorbing boundary conditions for water wave simulation in the vicinity of a solid body

J. M. Orellana,
M2N, Departement of mathematics, Conservatoire des Arts et Métiers
292, rue Saint Martin 75141 PARIS Cedex 03
France

Abstract- In this paper, we focus on the modelling of the wake of a solid body moving through a body of water. To this end, the flow of an inviscid, barotropic and compressible fluid around the solid body regarded as motionless is examined. The dynamic behaviour of the fluid is analysed by means of a two-dimensional Neumann-Kelvin's coupled model enhanced with capillarity and inertia terms. For computational purposes, the unbounded spatial domain must be truncated by artificial boundaries. Difficulties arise when it comes to setting appropriate absorbing boundary conditions for a waves propagation problem in a stratified convective fluid media with significant differences between layer properties. Numerical illustrations of the results are given and commented.

Keywords- Absorbing boundary conditions, fluid-structure interaction, water wave propagation, numerical simulations.

I. INTRODUCTION

WAVE propagation mechanisms on a body of water has long been a subject of interest for many researchers [4], [11], [13], [14]. Surface water wave phenomenon is due to the balance between the gravity forces that keep horizontal free surface of the water, the surface tension that keeps the consistency of the air-water interface, the water inertia and the difference between air and water pressure. According to the relevant effect that forces the motion, the waves are usually divided in gravity waves, capillary waves or pressure waves. Unlike conventional approaches, in our case the waves are regarded as interfacial gravity-capillary waves propagating between two liquid layers with very different properties. The upper layer is the free surface water with an infinitesimal thickness and small characteristic velocity of wave propagation namely, riddle velocity. The lower layer is the inner water with a finite or semi infinite thickness and an high characteristic velocity of wave propagation namely the speed of sound in water. The waves are usually generated by the movement of the solid body, interacting with its rigid surface and propagating all around it, leading to a wake in its vicinity.

After stating the problem and specifying underlying assumptions, a two dimensional Neumann-Kelvin's coupled modelization enhanced with capillarity and inertia terms is proposed [5]. A linearization around a steady state is performed and different accurate boundary conditions are introduced to carry out the study in open domain artificially bounded for computational limitation reasons. The variational formulation of the problem is deduced and a finite element approximation in space with a centered finite difference scheme in time are used to approach the solution. Results obtained by non-reflective boundary conditions are presented and discussed.

II. PROBLEM STATEMENT

Our purpose is to determine the dynamical behaviour of the water surface in the vicinity of a solid body that moves with an horizontal velocity U and with a possible oscillatory displacement. To this end, we examine the flow irrotational and inviscid of a compressible and barotropic fluid around the structure seen as fixed. Due to the existence of singularities at contact points between surface solid body and surface of water and at underwater angular points [6], the structure is immersed and its shape is simplified to a cylinder. We consider as computational domain a rectangular open domain Ω with an hole of radius R in its center. Its boundary $\partial\Omega = \Gamma_0 \cup \Gamma_1 \cup \Gamma_s \cup \Gamma_2 \cup \Gamma_b$ has unit outward normal vector ν . Γ_0 correponds to the bottom of the system, Γ_s , to the free surface of the water, Γ_1 and Γ_2 , to the sides through which the water flow enters and leaves Ω and Γ_b , to the rigid body surface (see Fig. 1). $\partial\Gamma_s$ denotes the edges of Γ_s . For numerical computations, the following values are set $L = 1 m, H = 1 m, R = 5.10^{-2} m, U = 0.15 m.s^{-1}$. A steady flow passes through Ω with horizontal velocity U and a small disturbance is introduced in the fluid to initiate propagation phenomenon.

III. THEORETICAL MODELLING

In most cases, to address wave propagating problem in a body of water, common formulation is to find the velocity potential Φ and the vertical displacement of the surface η satisfying:

- The Laplace's equation

$$\Delta\Phi = 0 \text{ in } \Omega \times]0, T[, \quad (1)$$

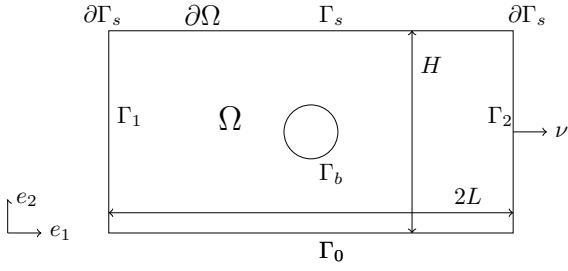


Fig. 1: Geometry and notations of the problem.

- The kinematic boundary conditions

$$\frac{\partial \Phi}{\partial \nu} = U \cdot \vec{\nu} \quad \text{on } \Gamma_0 \cup \Gamma_b \times]0, T[\quad (2)$$

$$\frac{\partial \Phi}{\partial \nu} = \frac{\partial \eta}{\partial t} + \nabla_s \Phi \cdot \nabla_s \eta \quad \text{on } \Gamma_s \times]0, T[, \quad (3)$$

- The dynamic boundary conditions

$$\frac{\partial \Phi}{\partial t} - \frac{1}{2} \|\nabla_s \Phi\|^2 - g\eta = 0 \quad \text{on } \Gamma_s \times]0, T[, \quad (4)$$

- The radiation boundary conditions based on the behavior of the solution in the neighborhood of infinity.

$$\nabla \Phi \rightarrow 0 \quad \text{as } |x| \rightarrow \infty, \quad t \in]0, T[, \quad (5)$$

Incompressibility of the flow is assumed and capillarity of the surface is neglected thereby greatly simplifying the formulation. In this study, a wave propagation problem with an uniform mean flow in an unbounded stratified fluid waveguide is considered. The propagating medium considered consists of two liquid layers with very different properties and then two models have to be introduced to take these features into account: an inner fluid model and a surface model. The global non-linear dynamical model obtained is linearized around a main steady state. Therefore the global solution is split into the steady state obtained and a transient one. The lateral boundary conditions are defined separately according to the nature of the state. For the steady flow, the most realistic condition is to fix the normal velocity. For transient flow, non-reflecting boundary conditions (NRBC) have to be prescribed for the inlet and the outlet of Ω in order to avoid any spurious rebounds of the waves reaching the boundaries of the domain.

Hypotheses and formulation of the global model

Formulation of the inner fluid model

We assume that the flow is characterized by two variables modelling the mass density ρ_{tot} and the velocity potential Φ that satisfy:

- the conservation of mass equation,

$$\frac{\partial \rho_{tot}}{\partial t} + \text{div}(\rho_{tot} \nabla \Phi) = 0 \quad \text{in } \Omega \times]0, T[, \quad (6)$$

- the Bernoulli equation for unsteady compressible potential flow (neglecting gravity effect),

$$\frac{\partial \Phi}{\partial t} + \frac{1}{2} \|\nabla \Phi\|^2 + F(\rho_{tot}) = 0 \quad \text{in } \Omega \times]0, T[\quad (7)$$

where $F(\rho_{tot}) = \int_{\rho_0}^{\rho_{tot}} \frac{1}{\rho} \frac{\partial p}{\partial \rho} d\rho + F(\rho_0)$ is the barotropic potential, p , the fluid pressure and T , the simulation time.

Formulation of the surface model

Applying Newton's second law of motion to a infinitesimal small surface element of thickness 2ε that vertically moves η_{tot} , leads to the free surface equilibrium equation:

$$2\varepsilon \rho_{tot} \frac{D^2 \eta_{tot}}{Dt^2} = -\rho_{tot} \frac{\partial \Phi}{\partial t} - \frac{\rho_{tot}}{2} \|\nabla_s \Phi\|^2 + \sigma \Delta_s \eta_{tot} - \rho_{tot} g \eta_{tot} \quad \text{in } \Gamma_s \times]0, T[, \quad (8)$$

where the forces involved consist in the capillary action $\sigma \Delta_s \eta_{tot}$, the gravity force $-\rho_{tot} g \eta_{tot}$ and the pressure $-\rho_{tot} \frac{\partial \Phi}{\partial t} - \frac{\rho_{tot}}{2} \|\nabla_s \Phi\|^2$. From a mathematical point of view, capillary term stabilizes the partial differential equation [5]. For water, the surface tension σ is equal to 0.075 N.m^{-1} and ε is set to 10^{-3} m . The subscript s indicates that the differential operator is considered locally along a surface namely here Γ_s .

On the interface

The continuity of normal velocity at the interface leads to the relation:

$$\frac{\partial \eta_{tot}}{\partial t} + \nabla_s \Phi \cdot \nabla_s \eta_{tot} = \frac{\partial \Phi}{\partial \nu} \quad \text{in } \Gamma_s \times]0, T[, \quad (9)$$

taking account of the rotation of the normal to the surface.

Linearization of the governing equations

Main background steady state flow

We introduce φ_0 , the velocity potential of the main steady state flow. It corresponds to a steady quasi-uniform horizontal flow of an incompressible fluid which enters and leaves Ω at constant unit horizontal velocity with normal surface displacement variation along Γ_s regarded as negligible and non penetrability condition on $\Gamma_0 \cup \Gamma_b$ satisfied. This background flow is stationary with respect to the solid which is chosen as frame of reference.

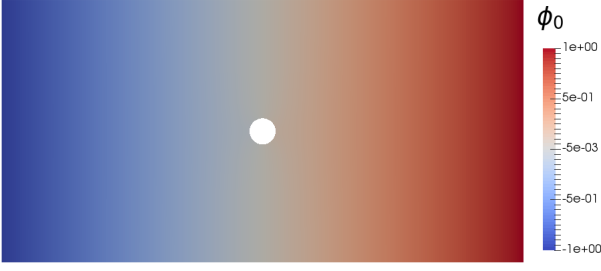


Fig. 2: Velocity potential φ_0 solution of (10) in Ω .

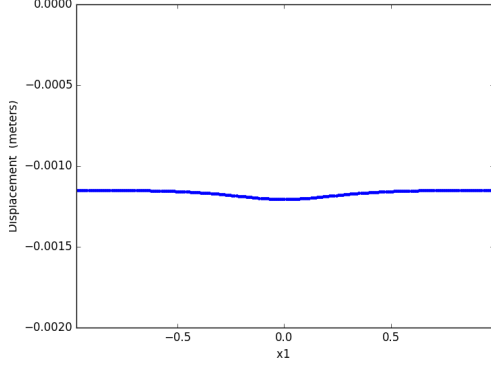


Fig. 3: Free surface vertical displacement η_0 solution of (11) with ‘digging’ effect.

φ_0 is the solution to the following problem :

$$\begin{cases} -\Delta\varphi_0 = 0, & \text{in } \Omega \text{ and } \int_{\Gamma_s} \varphi_0 = 0, \\ \frac{\partial\varphi_0}{\partial\nu} = 0, & \text{on } \Gamma_0 \cup \Gamma_b \cup \Gamma_s, \\ \frac{\partial\varphi_0}{\partial\nu} = (e_1 \cdot \nu) & \text{in } \Gamma_1 \cup \Gamma_2, \end{cases} \quad (10)$$

To evaluate corresponding surface displacement η_0 of this main flow, stationary balance of forces on free surface together with homogenous Neumann boundary conditions are applied. According to the frame of reference, it lead in stationary case to

$$\begin{cases} 2\varepsilon\rho_0 U^2 \nabla_s \varphi_0 \cdot \nabla_s (\nabla_s \varphi_0 \cdot \nabla_s \eta_0) = \\ -\sigma \Delta_s \eta_0 + \rho_0 g \eta_0 - \frac{\rho_0}{2} U^2 \|\nabla_s \varphi_0\|^2 & \text{in } \Gamma_s, \\ \frac{\partial\eta_0}{\partial\nu_s} = 0 & \text{on } \partial\Gamma_s \end{cases} \quad (11)$$

with $\rho_0 = 10^3 \text{kg.m}^{-3}$ and $g = 9.8 \text{m.s}^{-2}$. The solution corresponds to a steady quasi uniform horizontal flow with a digging effect due to the term $-\rho_0 U^2 \|\nabla_s \varphi_0\|^2 / 2$ (see Fig. 2 and 3). The order of magnitude of free surface strain is about 10^{-3}m and therefore negligible in comparison with initial computational domain Ω dimensions.

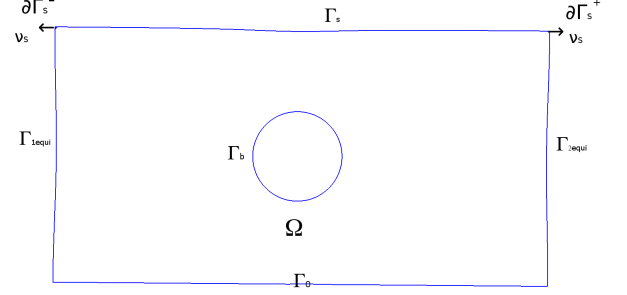


Fig. 4: Calculated geometry of the new computational domain in the case of a solid body size large compared to initial computational domain. The digging effect on Γ_s and the inwards bowing of Γ_{1equi} and Γ_{2equi} are more pronounced than in our case.

Transient state

We study the evolution of a small disturbance around the steady state $(\rho_0, \varphi_0, \eta_0)$. The unsteady waves in the fluid are represented by the perturbation functions ρ, φ, η of variables $x(x_1, x_2)$ and t . The problem is formulated with them wherein $\rho_{tot}(x, t) = \rho_0(x) + \rho(x, t)$, $\Phi(x, t) = U\varphi_0(x) + \varphi(x, t)$, $\eta_{tot}(x, t) = \eta_0(x) + \eta(x, t)$. The solution is split into main background steady state component and a transient one. The domain Ω is then cropped by $\Gamma_0, \Gamma_b, \Gamma_s = \eta_0, \Gamma_{1equi}$ and Γ_{2equi} [3]. The new lateral boundaries Γ_{1equi} and Γ_{2equi} correspond to equipotential lines of φ_0 passing respectively through left upper domain corner and right upper corner of Ω . The artificial boundaries are chosen far enough from rigid body to consider that steady state flow is uniform in this area and so the corners of the new domain are right-angled. The disturbance is so small that it is then reasonable to neglect the non-linear terms in the governing equations. Hence (ρ, φ, η) satisfy the linearized enhanced Neumann-Kelvin’s model with capillarity:

- the linearized continuity equation,

$$\frac{\partial\rho}{\partial t} + U\nabla\rho \cdot \nabla\varphi_0 + \rho_0\Delta\varphi = 0 \quad \text{in } \Omega \times]0, T[; \quad (12)$$

- the linearized momentum equation for the inner fluid,

$$\frac{\partial^2\varphi}{\partial t^2} + 2U\nabla\varphi_0 \cdot \nabla\left(\frac{\partial\varphi}{\partial t}\right) + U^2\nabla\varphi_0 \cdot \nabla(\nabla\varphi_0 \cdot \nabla\varphi) - c_f^2\Delta\varphi = 0 \quad \text{in } \Omega \times]0, T[\quad (13)$$

obtained from (7) and (12) given that $\frac{1}{2}|\nabla\varphi_0|^2 +$

$$\nabla F(\rho_0) = 0 \text{ and } \frac{\partial F(\rho_0)}{\partial\rho_{tot}} = \frac{c_f^2}{\rho_0};$$

- the linearized momentum equation for the surface fluid,

$$\begin{aligned}
& 2\varepsilon\rho_0 \left(\frac{\partial^2 \eta}{\partial t^2} + 2U\nabla_s \varphi_0 \cdot \nabla_s \frac{\partial \eta}{\partial t} \right) + \\
& 2\varepsilon\rho_0 (U^2 \nabla_s \varphi_0 \cdot \nabla_s (\nabla_s \varphi_0 \cdot \nabla_s \eta)) \\
& = \sigma \Delta_s \eta - \rho_0 g \eta - \rho_0 \frac{\partial \varphi}{\partial t} - \rho_0 U \nabla_s \varphi_0 \cdot \nabla_s \varphi \\
& \quad \text{in } \Gamma_s \times]0, T[. \quad (14)
\end{aligned}$$

where \cdot denotes the scalar product. Since the domain of study is reshaped, $\nabla_s \eta_0$ and $\Delta_s \eta_0$ are set to zero on Γ_s .

- the continuity of normal velocity at the interface

$$\frac{\partial \varphi}{\partial \nu} = \frac{\partial \eta}{\partial t} + U \nabla_s \varphi_0 \cdot \nabla_s \eta \quad \text{in } \Gamma_s \times]0, T[; \quad (15)$$

- the non-penetrability condition leads to homogeneous Neumann boundary condition for φ ,

$$\frac{\partial \varphi}{\partial \nu} = 0 \quad \text{in } \Gamma_0 \cup \Gamma_b \times]0, T[; \quad (16)$$

- initial conditions corresponding to a disturbance taking place on the inner fluid where functions $\varphi(x, 0)$ and $\frac{\partial \varphi}{\partial t}(x, 0)$ in Ω are prescribed.

Lateral artificial boundary conditions

Finding appropriate artificial boundary conditions able to handle unbounded problems has been an important subject of ongoing research. The main concern is that non-reflecting boundary condition should accurately represents the solution in the infinite domain outside for the arbitrary bounded domain of study [9]. Absorbing Boundary Conditions [8], [10] or Perfectly Match Layer techniques [1], [2] result in our case in multiplying the number of equations to solve, not to mention the existence of a background flow that increasing the difficulty of the problem .

Non-reflecting boundary condition imposed in the following on inner fluid lateral edges is :

$$\frac{\partial \varphi}{\partial t} + \left(U \frac{\partial \varphi_0}{\partial \nu} + c_f \right) \frac{\partial \varphi}{\partial \nu} = 0 \quad \text{in } \Gamma_{1equi} \cup \Gamma_{2equi} \times]0, T[\quad (17)$$

where c_f denotes the speed of sound in the fluid, $c_f = 10^3 m.s^{-1}$. These relation is consistent with Sommerfeld-like non reflecting boundary condition for a single wave which propagates at the phase velocity c_f corrected by taking account the normal to the boundary velocity component of the main background steady flow $U \frac{\partial \varphi_0}{\partial \nu}$. As lateral boundaries correspond to equipotential lines of φ_0 , the tangential to the boundary entry velocity of the main steady flow, $\nabla_s \varphi_0$, is equal to

zero and then it is assumed that main propagating phenomenon takes place along the normal to the boundary.

On the surface bounds $\partial \Gamma_s$ non-reflecting conditions imposed is the natural Sommerfeld-like non reflecting boundary condition,

$$\frac{\partial \eta}{\partial t} + \left(U \frac{\partial \varphi_0}{\partial \nu_s} + c_r \right) \frac{\partial \eta}{\partial \nu_s} = 0 \quad \text{on } \partial \Gamma_s, \quad \forall t \in]0, T[\quad (18)$$

where c_r denotes the riddle velocity with $c_r^2 = \frac{\sigma}{2\rho_0\varepsilon}$. It is consistent with the one-dimensional NRBC for a propagating wave at velocity c_r in an uniform background steady flow of velocity $U \frac{\partial \varphi_0}{\partial \nu_s}$. This boundary condition introduce a mathematical specific damping on each boundary nodes of the surface Γ_s in order to attenuate spurious reflecting modes.

IV. SOLUTION METHOD

Variational formulation and numerical approach

Multiplying (13) by $\psi \in H^1(\Omega)$ and (14) by $v \in H^1(\Gamma_s)$ respectively together with Green's formula application lead to a complicated coupled variational formulation of the problem not shown here for sake of clarity. Physical field approximation is performed by classical finite element method. A finite dimension subspace $V_h \subset H^1(\overline{\Omega})$ made of piecewise linear functions on a fixed mesh, characterized by element length h , is considered. Letting $V_h = span(\varphi_1, \varphi_2, \dots, \varphi_{N1}, \eta_1, \eta_2, \dots, \eta_{N2})$ with φ_i $1 \leq i \leq N1$ and η_i $1 \leq i \leq N2$ finite element shape functions on Ω and on Γ_s respectively. Calling X the coordinate vector of \mathcal{X} relative to this basis lead to the recasted algebraic differential linear problem : Find $X(t) \in R^N$, $N = N1 + N2$, $t \in]0, T[$ such that

$$M\ddot{X} + C\dot{X} + KX = 0 \quad (19)$$

with $X(0), \dot{X}(0)$ prescribed. M, C, K are sparces matrices VI. Centered finite difference scheme is applied for the time domain approximation in order to avoid numerical instabilities. Finally the problem becomes: Find $X \in R^{N1}$ such that

$$A_1 X^{(n+1)} = A_2 X^{(n)} + A_3 X^{(n-1)} \quad (20)$$

where A_1, A_2 et A_3 are sparces matrices depending on M, C, K and Δt with Δt the time step chosen VI. Meshes are generated by GMSH. Due to the complexity of weak formulation terms, low-level generic assembly procedures of python module of GETFEM++ is employed to make the assembly of the involved sparces matrices in (19). To compute the solution of the large sparse system (20) a MUMPS solver is used. Mesh convergence study performed by reducing characterisitic size of elements of the from $h = 1e - 3$ to $h = 6.25e - 5$. As shown in Fig. 5 and and Fig. 6, results converge upon

a solution as the mesh density increased. A satisfactory balance between accuracy of results and computing time consuming can be achieved by choosing the value of $h = 1.25e - 4$. Surface vertical displacement η_0 and equipotential lines Γ_{1equi} and Γ_{2equi} are extracted from steady state flow simulation results to generate the new computational domain Ω .

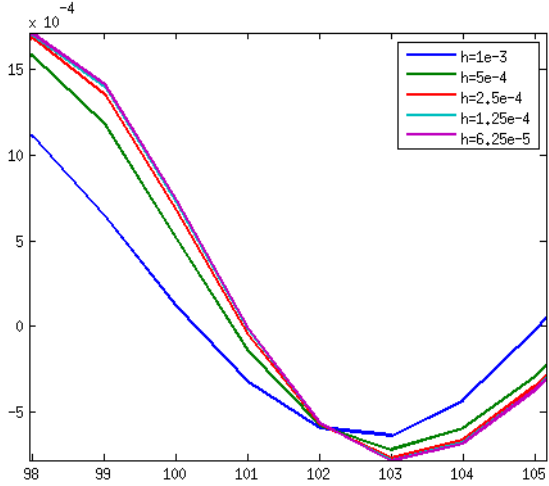


Fig. 5: Inner fluid potential φ results at point of coordinates $(0.5, 0.5)$ versus time in $10^{-5}s$ for different elements size of the mesh.

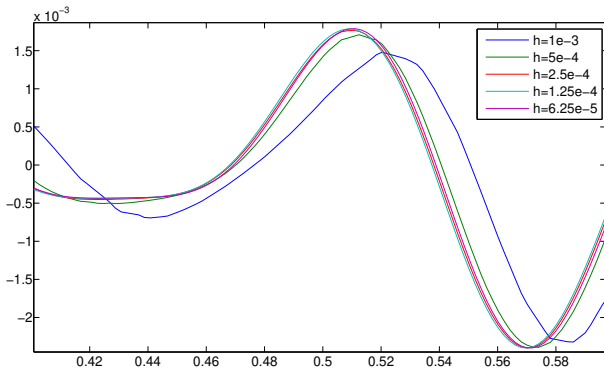


Fig. 6: Inner fluid potential φ results for different mesh densities along the middle line of computational domain on $[0.4, 0.6]$ at $10^{-3}s$.

V. RESULTS AND COMMENTS

Wave propagation phenomenon is monitored by the variation of φ in the inner fluid and the variation of η on the surface respectively. The value of time step chosen is $\Delta t_v = 10^{-5}s$ in order to see properly wave propagation with a velocity of c_f across the extend of the computational domain Ω . As it can be seen on figures (see Fig. 7) reflecting waves appear on the bottom of the domain just like on the surface of the immersed solid

body where homogeneous Neumann conditions are imposed to modelize non penetrability of the fluid through them. On both lateral side of the computational domain no spurious reflecting wave appears to be present (see Fig. 7). Thanks to hyperbolicity of the problem, in order to verify whether NRBC are satisfactory on inner fluid lateral edges (17), a similar study is carried out according to the same previous calculation criteria on a more expanded computational domain in x direction sized so as to avoid lateral side spurious reflecting waves on the time range analysed. The new solution obtained is regarded as a reference solution. Both resulting waves are in phase but a variable amplitude difference can be noticed (see Fig. 8). The wave is slightly reflected especially on its peak of amplitude and at times when there are not many interferences.

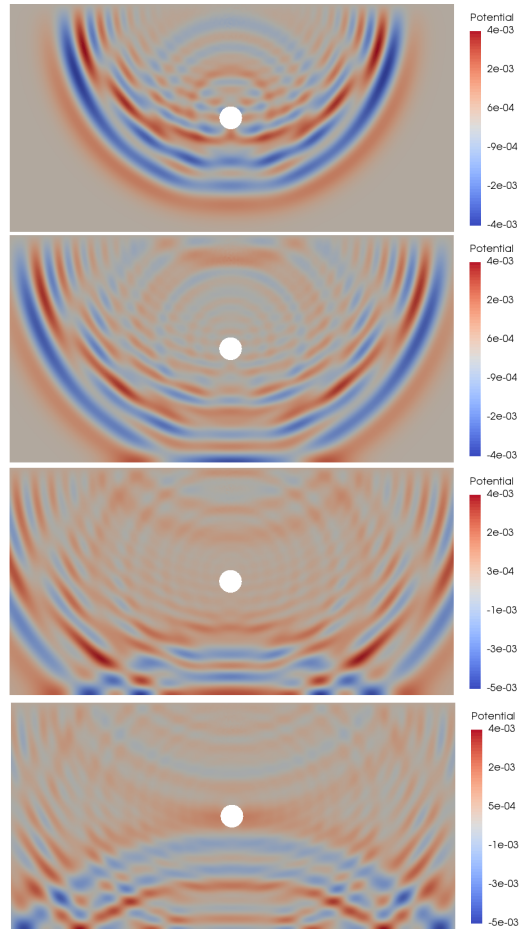


Fig. 7: Propagation of disturbance φ at times: $t = 80\Delta t_v$, $t = 100\Delta t_v$, $t = 120\Delta t_v$, $t = 140\Delta t_v$. Its order of magnitude is $10^{-1}m^2s^{-1}$;

Waves propagation in inner fluid results in deformation of the surface as shown in Fig. 9 and 10. The corresponding normal displacement η propagates along the surface Γ_s . On each side of the surface, $\partial\Gamma_s$, no spurious reflective wave is noticed. In inner fluid layer no wave related with any reflective surface on surface is neither observed (see Fig. 10). Then lateral boundary conditions introduced (18) seem to be also adequate to

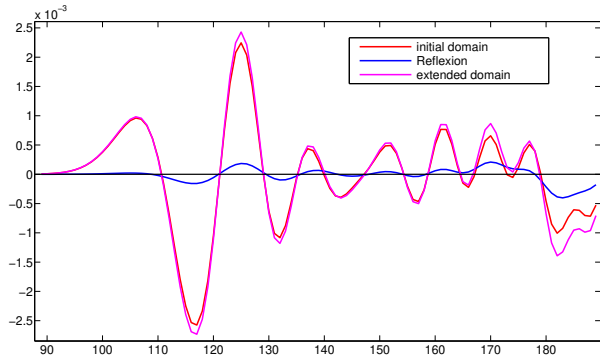


Fig. 8: Comparison of inner fluid potential φ results versus time in $10^{-5}s$ between extended and main computational domain on the middle of right artificial lateral edge.

successfully modelize the propagating phenomenon on the surface [3]. Nevertheless the velocity of the phenomenon is the same as in inner fluid layer which is not in complete agreement with surface layer material properties and wave propagation in stratified media theories. The expected value should be closed to the riddle velocity, c_r . Therefore no surface propagation phenomenon should be observed with time step Δt_v . That's actually what happens where initial disturbances are located just below the surface or on the surface itself as shown in Fig. 11 and 12. In order to observe surface wave propagation in this last case a time step $\Delta t_s = 10^{-2}s$ must be chosen. Moreover due to the significant difference between the wave propagation velocity values of the surface and inner fluid layers, singularities should appear on the intersection between the artifically chosen boundaries of the domain and the two layers interface [7]. This result is confirmed by numerical simulation in the case of an initial disturbance of the surface with a non zero initial value to η as it can be seen in Fig. 14. The non reflecting boundary condition on the lateral edges (14) has to be changed to handle this difficulties [12]. At last, in order to verify this result, numerical simulations with a reflective homogenous Dirichlet boundary conditions $\eta = 0$ were applied on both edges of the surface and no reflective surface wave was neither noticed. To sum things up, the observed normal displacements η in Fig. 9 and 10 are not related directly to surface wave propagation, but rather primarily related to the potential volume wave propagation in inner fluid layer and to the interface coupling between the potential φ and the normal displacement η on Γ_s given by (15). The energy transmitted to the surface layer by the inner layer remains stationary over the time range considered. Therefore application of lateral boundary conditions (18) does not measurably affect the propagation phenomenon and its accuracy can't be estimated with a disturbance in inner fluid layer.

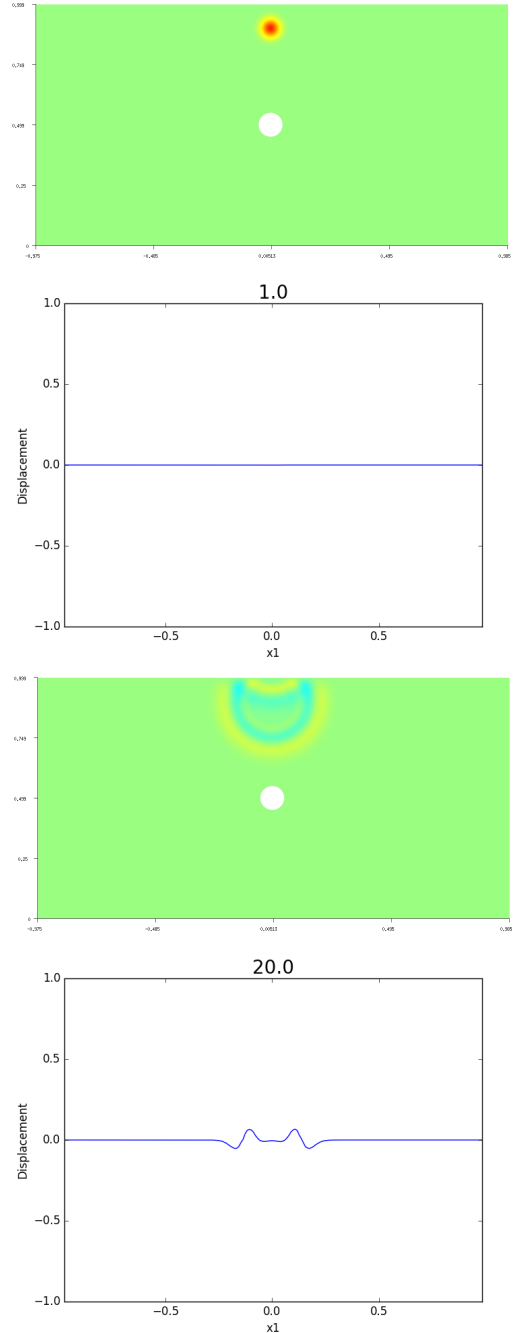


Fig. 9: Propagation of disturbance φ in Ω and related normal surface displacement η on Γ_s versus x_1 coordinate at times: $t = \Delta t_v$, $t = 20\Delta t_v$. Its order of magnitude is $10^{-1}m^2s^{-1}$ and order of magnitude of the normal displacement is $10^{-5}m$.

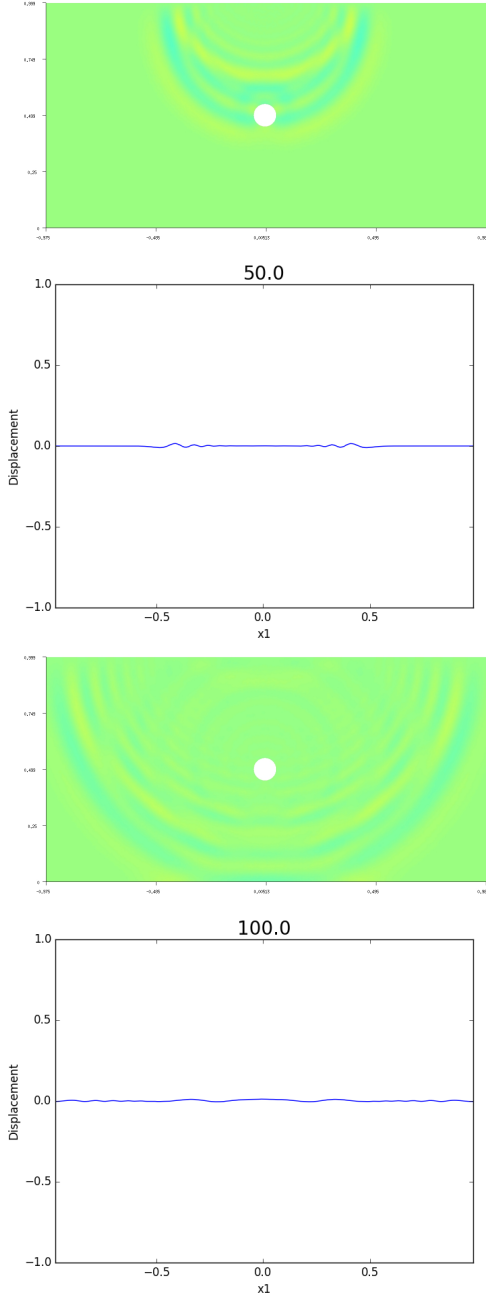


Fig. 10: Propagation of disturbance φ in Ω and related normal surface displacement η on Γ_s versus x_1 coordinate at times: $t = 50\Delta t_v$, $t = 100\Delta t_v$. Its order of magnitude is $10^{-1}m^2s^{-1}$ and corresponding normal displacement η order of magnitude is $10^{-5}m$.

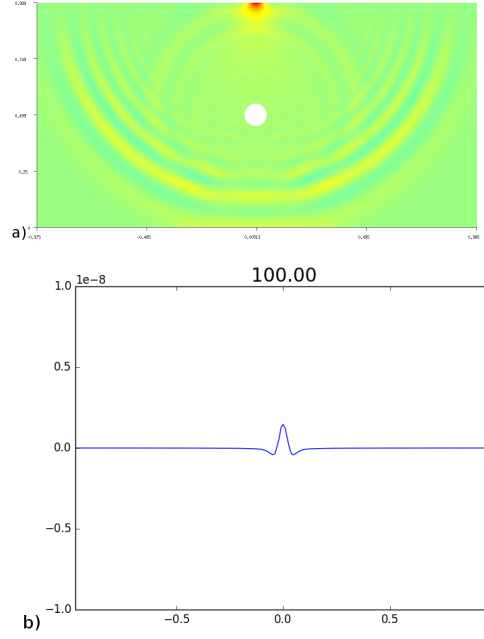


Fig. 11: Propagation of potential disturbance φ in Ω (a) and related normal surface displacement η (b) on Γ_s versus x_1 coordinate at times $t = 100\Delta t_v$. Initial disturbance is located in the inner fluid just below the surface and its order of magnitude is $\varphi = 10^{-7}m^2s^{-1}$. Stationary corresponding normal displacement order of magnitude is $10^{-9}m$.

VI. CONCLUSION

For the modelling of the wake of a solid body in the water, a wave propagation problem in a stratified media is considered. In order to apply standard methods of resolution intended for bounded domains, artificial boundaries are introduced and appropriate local non-reflecting boundary conditions are devised. However the significant differences between layer properties make it difficult to address the entire problem. Nevertheless this work has shown a surface phenomenon related to a bulk waves propagation in water which is let aside by incompressibility hypothesis in common study and has also allowed to devise a new appropriate boundary condition for waves propagation problems in stratified convective media. Further works focused on surface waves propagation have to be carried out and singularities has to be handled in this case.

APPENDIX

Algebraic differential linear problem sparses matrix expressions :

$$M = \begin{bmatrix} M_{ff} & 0 \\ 0 & M_{ss} \end{bmatrix}$$

$$\text{with } M_{ff} = \int_{\Omega} \varphi \psi d\tau \text{ and } M_{ss} = 2\varepsilon c_f^2 \int_{\Gamma_s} \eta v d\sigma.$$

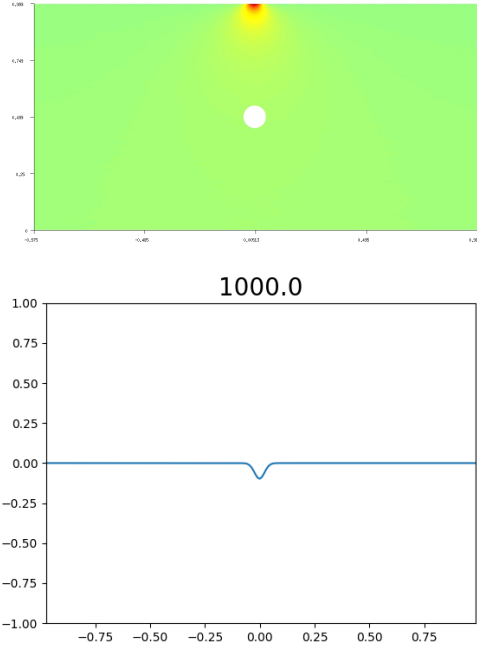


Fig. 12: Propagation of normal surface displacement η on Γ_s and related disturbance φ in Ω at time $t = 1000\Delta t_v$. Initial disturbance is located on the surface of the fluid. The order of magnitude of η is $10^{-6}m$. The order of magnitude of the potential φ transmitted to the inner fluid is $10^{-7}m^2s^{-1}$.

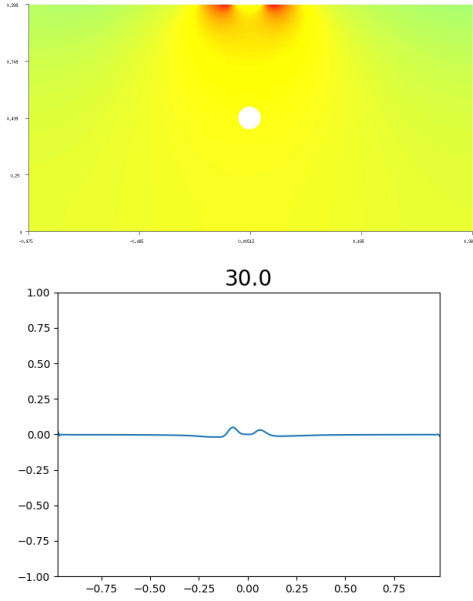


Fig. 13: Propagation of normal surface displacement η on Γ_s and related disturbance φ in Ω at time $t = 30\Delta t_s$. Initial disturbance is located on the surface of the fluid. Its order of magnitude is $10^{-6}m$.

$$C = \begin{bmatrix} C_{ff} & C_{fs} \\ C_{sf} & C_{ss} \end{bmatrix},$$

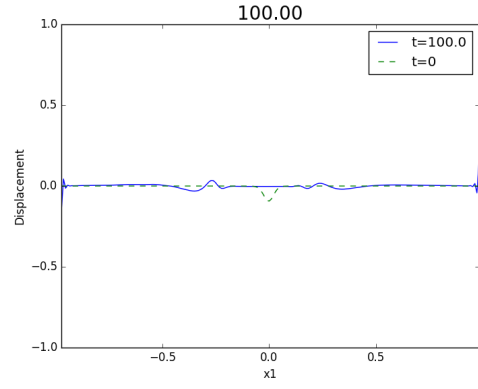


Fig. 14: Disturbance η of the surface Γ_s at time $t = 100\Delta t_s$ versus x_1 coordinate. Initial disturbance is located on the surface Γ_s in dash point. Singularities appear on the edge of the surface, $\partial\Gamma_s$.

$$\begin{aligned} \text{with } C_{ff} &= U \int_{\Omega} \nabla\varphi_0 \cdot (\nabla\varphi\psi - \varphi\nabla\psi) d\tau + c_f \int_{\Gamma} \varphi\psi d\sigma, \\ C_{fs} &= -c_f^2 \int_{\Gamma_s} \eta\psi d\sigma, \quad C_{sf} = c_f^2 \int_{\Gamma_s} \varphi v d\sigma \text{ and} \\ C_{ss} &= 2\varepsilon c_f^2 U \int_{\Gamma_s} (\nabla_s\varphi_0 (\nabla_s\eta v - \eta\nabla_s v) - v\Delta_s\varphi_0\eta) d\sigma \\ &\quad + [2\varepsilon c_f^2 c_r \eta v]_{\partial\Gamma_s}. \end{aligned}$$

$$K = \begin{bmatrix} K_{ff} & K_{fs} \\ K_{sf} & K_{ss} \end{bmatrix},$$

with

$$K_{ff} = c_f^2 \int_{\Omega} (\nabla\varphi \cdot \nabla\psi - U^2 (\nabla\varphi_0 \cdot \nabla\varphi) (\nabla\varphi_0 \cdot \nabla\psi)) d\tau,$$

$$K_{fs} = -c_f^2 U \int_{\Gamma_s} \nabla_s\varphi_0 \cdot \nabla_s v \varphi d\sigma + \left[c_f^2 U \frac{\partial\varphi_0}{\partial\nu_s} \varphi v \right]_{\partial\Gamma_s},$$

$$K_{sf} = -c_f^2 U \int_{\Gamma_s} \nabla_s\varphi_0 \cdot \nabla_s v \varphi d\sigma$$

and

$$K_{ss} = -2\varepsilon c_f^2 U^2 \int_{\Gamma_s} ((\nabla_s\varphi_0 \cdot \nabla_s\eta) (\nabla_s\varphi_0 \cdot \nabla_s v)) d\sigma$$

$$- 2\varepsilon c_f^2 U^2 \int_{\Gamma_s} (-v\Delta_s\varphi_0 (\nabla_s\varphi_0 \cdot \nabla_s\eta)) d\sigma$$

$$+ \frac{c_f^2}{\rho_0} \int_{\Gamma_s} (\sigma \nabla_s\eta \cdot \nabla_s v + \rho_0 \eta g v) d\sigma.$$

Differential terms $d\tau$ or $d\sigma$ indicate that integration is taken with respect to area or with respect to arc length respectively. Subscript f and s stand for inner fluid

and surface fluid respectively. φ and ψ are equal to φ_i $1 \leq i \leq N_1$. η and v are equal to η_i $1 \leq i \leq N_2$.

$$A_1 = M + \frac{C}{2}\Delta t + \frac{K}{2}\Delta t^2,$$

$$A_2 = 2M,$$

$$A_3 = -M + \frac{C}{2}\Delta t - \frac{K}{2}\Delta t^2.$$

wherein M , C and K have the above meanings and Δt the time step used in the numerical simulation.

ACKNOWLEDGMENT

I would like to thank Professor Philippe Destuynder, emeritus professor of University of La Rochelle, France (Laboratory LaSIE) for fruitful discussions.

REFERENCES

- [1] BÉCACHE, E., DHIA, A. B.-B., AND LEGENDRE, G. Perfectly matched layers for the convected helmholtz equation. *SIAM Journal on Numerical Analysis* 42, 1 (2004), 409–433.
- [2] BERENGER, J.-P. A perfectly matched layer for the absorption of electromagnetic waves. *Journal of computational physics* 114, 2 (1994), 185–200.
- [3] BISSENGUE, D., AND WILK, O. Conditions aux limites transparentes et modélisation des vagues de surface dans un écoulement. Master’s thesis, EIC-NAM, 2012.
- [4] BREKHOVSKIKH, L. *Waves in layered media*, vol. 16. Elsevier, 2012.
- [5] DESTUYNDER, P., AND FABRE, C. A discussion on neumann–kelvin’s model for progressive water waves. *Applicable Analysis* 90, 12 (2011), 1851–1876.
- [6] DESTUYNDER, P., AND FABRE, C. Modélisation du comportement hydrodynamique des bateaux. Lecture, June 2012.
- [7] DESTUYNDER, P., AND FABRE, C. Singularities occurring in multimaterials with transparent boundary conditions. *Quarterly of Applied Mathematics* 74, 3 (June 2016), 443–463.
- [8] ENGQUIST, B., AND MAJDA, A. Absorbing boundary conditions for numerical simulation of waves. *Proceedings of the National Academy of Sciences* 74, 5 (1977), 1765–1766.
- [9] GIVOLI, D. *Numerical methods for problems in infinite domains*, vol. 33. Elsevier, 2013.
- [10] HALPERN, L. Absorbing boundary conditions for the discretization schemes of the one-dimensional wave equation. *Mathematics of Computation* 38, 158 (1982), 415–429.
- [11] LIGHTHILL, J. *Waves in fluids*. Cambridge university press, 2001.
- [12] LÓPEZ DE SILANES, M., ET AL. *Fourteenth International Conference Zaragoza–Pau on Mathematics and its Applications: Jaca (Spain), September 12*, vol. 41. Prensas de la Universidad de Zaragoza, 2018.
- [13] MILES, J. W. On the generation of surface waves by shear flows. *Journal of Fluid Mechanics* 3, 02 (1957), 185–204.
- [14] STOCKER, J. Water waves. *Pure and Applied Mathematics* 9 (1957), 291–314.